Elimination of GPI2 suppresses glycosylphosphatidylinositol GlcNAc transferase activity and alters GPI glycan modification in Trypanosoma brucei

Jenni, Aurelio; Knüsel, Sebastian; Nagar, Rupa; Benninger, Mattias; Häner, Robert; Ferguson, Michael A. J.

Published in:
Journal of Biological Chemistry

DOI:
10.1016/j.jbc.2021.100977

Publication date:
2021

JBC RESEARCH ARTICLE

Elimination of GPI2 suppresses glycosylphosphatidylinositol GlcNAc transferase activity and alters GPI glycan modification in *Trypanosoma brucei*

Received for publication, March 17, 2021, and in revised form, June 20, 2021 Published, Papers in Press, July 18, 2021,
https://doi.org/10.1016/j.jbc.2021.100977

Aurelio Jenni[1,2], Sebastian Knüsel[3], Rupa Nagar[4], Mattias Benninger[3], Robert Häner[5], Michael A. J. Ferguson[4], Isabel Roditi[3], Anant K. Menon[6], and Peter Bütikofer[1,*]

From the [1]Institute of Biochemistry and Molecular Medicine, [2]Graduate School for Chemical and Biomedical Sciences, [3]Institute of Cell Biology, University of Bern, Bern, Switzerland; [4]Wellcome Centre for Anti-Infectives Research, School of Life Sciences, University of Dundee, Dundee, United Kingdom; [5]Department for Chemistry and Biochemistry, University of Bern, Bern, Switzerland; [6]Department of Biochemistry, Weill Cornell Medical College, New York, New York, USA

Edited by Gerald Hart

Many eukaryotic cell-surface proteins are post-translationally modified by a glycosylphosphatidylinositol (GPI) moiety that anchors them to the cell membrane. The biosynthesis of GPI anchors is initiated in the endoplasmic reticulum by transfer of GlcNAc from UDP-GlcNAc to phosphatidylinositol. This reaction is catalyzed by GPI GlcNAc transferase, a multisubunit complex comprising the catalytic subunit Gpi3/PIG-A as well as at least five other subunits, including the hydrophobic protein Gpi2, which is essential for the activity of the complex in yeast and mammals, but the function of which is not known. To investigate the role of Gpi2, we exploited *Trypanosoma brucei* (Tb), an early diverging eukaryote and important model organism that initially provided the first insights into GPI structure and biosynthesis. We generated insect-stage (procyclic) trypanosomes that lack TbGPI2 and found that in TbGPI2-null parasites, (i) GPI GlcNAc transferase activity is reduced, but not lost, in contrast with yeast and human cells, (ii) the GPI GlcNAc transferase complex persists, but its architecture is affected, with loss of at least the TbGPI1 subunit, and (iii) the GPI anchors of procyclins, the major surface proteins, are underglycosylated when compared with their WT counterparts, indicating the importance of TbGPI2 for reactions that occur in the Golgi apparatus. Immunofluorescence microscopy localized TbGPI2 not only to the endoplasmic reticulum but also to the Golgi apparatus, suggesting that in addition to its expected function as a subunit of the GPI GlcNAc transferase complex, TbGPI2 may have an enigmatic noncanonical role in Golgi-localized GPI anchor modification in trypanosomes.

Roughly 1% of all proteins encoded by eukaryotic genomes are post-translationally modified at their C terminus by glycosylphosphatidylinositol (GPI), a complex glycophospholipid that anchors the protein to the cell surface. Its core structure consists of ethanolamine-PO_4-6Manα1-2Manα1-6Manα1-4GlcNα1-6*myo*-inositol-1-PO_4-lipid, with the ethanolamine residue being linked to the C terminus of the protein *via* an amide bond (1). The glycan core can be extensively modified with phosphoethanolamine residues, monosaccharides, and/or oligosaccharides, depending on the protein and cell-type in question (2).

GPI anchoring occurs in the lumen of the endoplasmic reticulum (ER), but the biosynthesis of the glycolipid itself is initiated on the cytoplasmic side (3) by the addition of GlcNAc from UDP-GlcNAc to a *myo*-inositol-containing phospholipid, most commonly phosphatidylinositol (PI). In subsequent reactions, GlcNAc–PI is de-*N*-acetylated (4) to glucosamine (GlcN)–PI, which is then translocated across the ER membrane (5) by an unknown scramblase and modified by inositol acylation and addition of mannosyl and phosphoethanolamine residues to generate a GPI anchor precursor appropriately situated for transfer to newly translocated proteins (1, 2, 6). Species-specific and cell type–specific modifications of the GPI core structure then occur in the ER and Golgi apparatus and during transport of GPIs and GPI-anchored proteins to the cell surface (7–10).

The synthesis of GlcNAc–PI is catalyzed by UDP-GlcNAc–PI α1-6 GlcNAc-transferase (henceforth GPI GlcNAc transferase), a multisubunit, membrane-bound complex consisting of Gpi1/PIG-Q, Gpi2/PIG-C, Gpi3/PIG-A, Gpi15/PIG-H, Gpi19/PIG-P, and Eri1/PIG-Y (nomenclature corresponding to yeast/mammals) (11–20); in mammalian cells, a seventh subunit, Dpm2, has been reported (20). The multisubunit nature of this enzyme is unexpected and enigmatic. Although it is clear that Gpi3/PIG-A is the catalytic subunit (21, 22), the functions of the other subunits are not evident. We were intrigued by the Gpi2/PIG-C subunit, a highly hydrophobic membrane protein that is essential for GPI GlcNAc transferase activity in yeast and humans (11, 17, 23). It has been speculated that Gpi2/PIG-C might play a role in recruiting the hydrophobic lipid substrate, PI, to the GPI GlcNAc transferase complex and/or maintaining the architecture of the transferase complex. To explore these possibilities, we turned to the parasite causing human sleeping sickness, *Trypanosoma brucei*, which offers a number of genetic and biochemical

* For correspondence: Peter Bütikofer, peter.buetikofer@ibmm.unibe.ch.

advantages to study GPI anchoring, notably that GPI biosynthesis is not essential for the survival of *T. brucei* procyclic forms in culture (24, 25), thereby allowing convenient manipulation of the GPI pathway without compromising cell viability. Historically, the high abundance of GPIs and GPI-anchored proteins in trypanosomes made it possible to delineate the first complete structure of a GPI anchor in *T. brucei* bloodstream forms (26) and the corresponding anchors in insect stage (procyclic) forms (27–29) and elucidate the reaction sequences leading to their synthesis (30–34). Notably, the GPI anchors in *T. brucei* procyclic forms are among the most complex GPI structures identified to date, with unusually large side chains consisting of characteristic polydisperse-branched *N*-acetyllactosamine (Galβ1–4GlcNAc) and lacto-*N*-biose (Galβ1–3GlcNAc) units capped with sialic acid residues (27, 28). Several enzymes involved in GPI side-chain modification in *T. brucei* have been identified and characterized (7, 35–37).

The core subunits of the GPI GlcNAc transferase complex have been identified in *T. brucei* by bioinformatics (38) and quantitative proteomics (39): TbGPI1 (Tb927.3.4570), TbGPI2 (Tb927.10.6140), TbGPI3 (Tb927.2.1780), TbGPI15 (Tb927.5.3680), TbGPI19 (Tb927.10.10110), and TbERI1 (Tb927.4.780). TbDPM2 (Tb927.9.6440) is also listed in the *T. brucei* genome, but this may be a misannotation as the trypanosome dolichol phosphate mannose synthase, like its *Saccharomyces cerevisiae* counterpart, comprises a single protein, TbDPM1 (40).

To explore the role of TbGPI2, we deleted the gene in *T. brucei* procyclic forms and characterized the KO cells (TbGPI2-KO) using a variety of biochemical readouts. The results of our analyses were unexpected at multiple levels and showed that GPI GlcNAc transferase activity is reduced but not lost in TbGPI2-KO parasites, with the residual activity being sufficient to maintain production of GPI-anchored proteins. Although the GPI GlcNAc transferase complex persists in the absence of TbGPI2, its architecture is affected, with loss of at least the TbGPI1 subunit. Unexpectedly, we found that GPI anchors of the major surface glycoproteins are underglycosylated in the absence of TbGPI2, indicating the importance of this protein for reactions that are expected to occur in the Golgi apparatus and suggesting that TbGPI2 may possess a hitherto unknown noncanonical function in regulating GPI side-chain modification in the Golgi apparatus.

Results and discussion

TbGPI2 is not required for growth of T. brucei *procyclic forms*

To investigate the role of TbGPI2 in GPI biosynthesis in *T. brucei*, we used CRISPR/CRISPR-associated protein 9 (Cas9) to replace both alleles of TbGPI2 with antibiotic resistance cassettes in procyclic form parasites. One viable clone was obtained, and replacement of both TbGPI2 alleles with drug resistance cassettes was verified by PCR (Fig. S1*A*) and Southern blotting (Fig. S2*A*). Loss of TbGPI2 mRNA was verified by Northern blotting (Fig. S2*B*). The TbGPI2-KO parasites grew more slowly than the isogenic parental strain (SmOx P9), with a doubling time of ∼11 h compared with ∼9.4 h for parental cells (Fig. 1*A*). Slower growth of GPI-deficient procyclic cells has been reported previously in some instances, for example, after knocking out TbGPI13 or TbGPI10 (24, 41), but not TbGPI12 (25). Growth was restored by expressing an ectopic copy of TbGPI2 (TbGPI2-HA, bearing a C-terminal 3x HA tag) in the TbGPI2-KO parasites (Fig. 1*A*); integration of the ectopic copy was verified by PCR (Fig. S1*B*) and expression of HA-tagged TbGPI2 by SDS-PAGE/immunoblotting (Fig. S1*D*).

We next tested the ability of TbGPI2-KO parasites to synthesize GPIs. Trypanosomes were metabolically labeled with [^{3}H]-ethanolamine, and GPI anchor precursors and free GPIs (Fig. 1*B*) were sequentially extracted and analyzed by TLC. Unexpectedly, extracts containing GPI precursors revealed the presence of a small amount of the GPI anchor precursor PP1 (<5% of that in parental cells) (Fig. 1*C*), suggesting residual GPI GlcNAc transferase activity in TbGPI2-KO parasites. This result contrasts with findings from *S. cerevisiae* (11) and human (17, 42) cells, where disruption of ScGPI2 and PIG-C, respectively, results in total loss of GPI GlcNAc transferase activity. In addition, we found that the levels of free GPIs—mature GPI anchors not attached to protein (43)—were decreased in TbGPI2-KO parasites compared with parental cells (Fig. 1*D*). Expression of TbGPI2-HA in the TbGPI2-KO background completely restored both PP1 and free GPI levels (Fig. 1, *C* and *D*), indicating that TbGPI2-HA is functional. We conclude that TbGPI2 has an important yet nonessential contribution to the activity of GPI GlcNAc transferase in *T. brucei*, such that a low level of GPI biosynthesis persists even in the absence of TbGPI2.

TbGPI2-KO-derived membranes are able to synthesize GlcNAc–PI

To quantify GPI GlcNAc transferase activity in TbGPI2-KO cells, we used a cell-free assay in which crude membranes are tested for their ability to generate [^{3}H]GlcNAc–PI from UDP-[^{3}H]GlcNAc and endogenous PI (30, 31, 33). TLC analyses of lipid extracts from such assays showed that both parental (Fig. 2*A*) and TbGPI2-KO (Fig. 2*B*)-derived membranes synthesized [^{3}H]GlcNAc–PI and the product of the subsequent reaction, [^{3}H]GlcN–PI. The assay with membranes from the parental parasites showed accumulation of [^{3}H]GlcNAc–PI (Fig. 2, *A* and *C*), indicating that conversion to [^{3}H]GlcN–PI is rate limiting. In contrast, in membranes from TbGPI2-KO cells, production of [^{3}H]GlcNAc–PI was sharply decreased (compare Fig. 2*B* *versus* Fig. 2*A*), and the ratio between [^{3}H]GlcNAc–PI and [^{3}H]GlcN–PI was shifted toward [^{3}H]GlcN–PI (Fig. 2, *B* and *D*). This result is consistent with a decreased rate of synthesis caused by a weakened GPI GlcNAc transferase enzyme, such that the first reaction is now the rate-limiting step. Together, these results show that GPI GlcNAc transferase activity is decreased, but not absent, in parasites lacking TbGPI2.

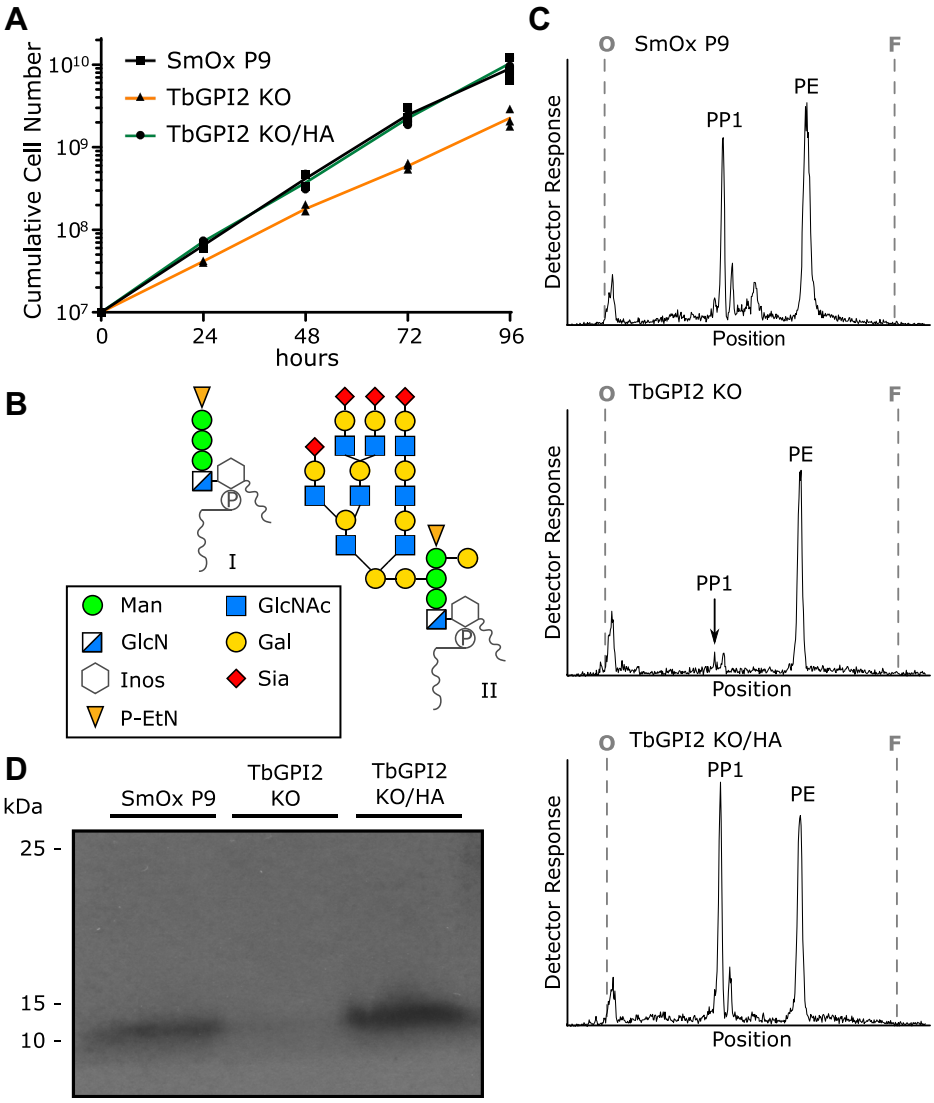

Figure 1. Characterization of TbGPI2-KO parasites. *A*, growth of *Trypanosoma brucei* SmOx P9 (*black line*), TbGPI2-KO (*red line*), and TbGPI2-KO/HA (TbGPI2-KO parasites expressing HA-tagged TbGPI2; *green line*) procyclic forms cultured under identical conditions. Data are from three independent experiments. *B*, schematic structures of GPI precursor PP1 (I) and free GPIs (II, taken from the procyclin GPI anchor). *C* and *D*, *T. brucei* SmOx P9, TbGPI2-KO, and TbGPI2-KO/HA were cultured for 16 h in the presence of [^{3}H]-ethanolamine and subjected to a sequential extraction protocol. GPI precursors and free GPIs were analyzed by TLC and radioisotope scanning (*C*; the extracts contain residual amounts of [^{3}H]-ethanolamine-labeled phosphatidylethanolamine (PE)), and SDS-PAGE followed by fluorography (*D*; molecular mass markers are indicated), respectively. F, solvent front; O, site of sample application.

TbGPI2-KO cells synthesize GPI-anchored procyclins with reduced apparent mass

Because TbGPI2-KO parasites have a low level of GPI GlcNAc transferase activity and synthesize PP1, albeit in low amounts, we next investigated whether they also synthesize the stage-specific GPI-anchored procyclins EP (44) and GPEET (45). Procyclins can be extracted from cells with 9% (v/v) n-butanol in water (27, 45), and they migrate on SDS-PAGE as a broad band at 22 to 32 kDa for GPEET, and at around 42 kD for EP, which is a relatively minor GPI-anchored protein in early procyclic forms (45–47). TbGPI2-KO and isogenic parental cells were metabolically labeled with [^{3}H]-ethanolamine and probed for radiolabeled procyclins by SDS-PAGE and fluorography. Parental cells (SmOx P9) showed a strong radiolabeled GPEET band, as well as a weak band corresponding to EP procyclin (Fig. 3*A*), and as expected (41), no labeled procyclins were detected in a control sample of *T. brucei* procyclic forms that lack TbGPI13, the enzyme that adds phosphoethanolamine to the third mannose of the GPI anchor. Interestingly, TbGPI2-KO cells showed a radiolabeled band with a lower apparent mass than GPEET procyclin in parental cells. This result suggests that GPI anchoring of GPEET occurs in TbGPI2-KO cells, but that some aspect of GPEET maturation is disrupted, resulting in a lower-molecular-weight form. Of note, we detected a radiolabeled 55-kDa protein in all three cell lines corresponding to ethanolamine phosphoglycerol-modified eukaryotic elongation

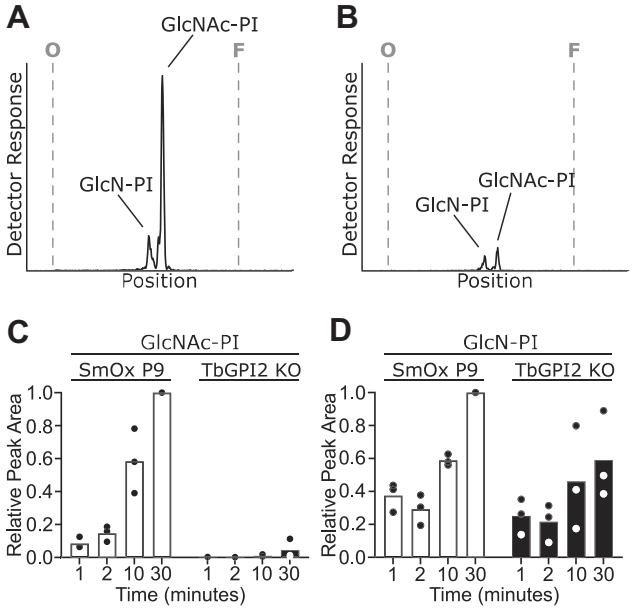

Figure 2. GPI GlcNAc transferase activity assayed in TbGPI2-KO membranes. *A* and *B*, membranes from *Trypanosoma brucei* SmOx P9 (*A*) and TbGPI2-KO (*B*) procyclic forms were incubated with UDP-[^{3}H]GlcNAc for 30 min, and lipids were extracted and analyzed by TLC and radioisotope scanning. *C* and *D*, quantification of time-dependent formation of [^{3}H]GlcNAc–PI (*C*) and [^{3}H]GlcN–PI (*D*) using the peak area from the chromatograms as readouts. Data from three independent experiments are shown, normalized to parental SmOx P9 cells, 30-min incubation time. F, solvent front; O, site of sample application.

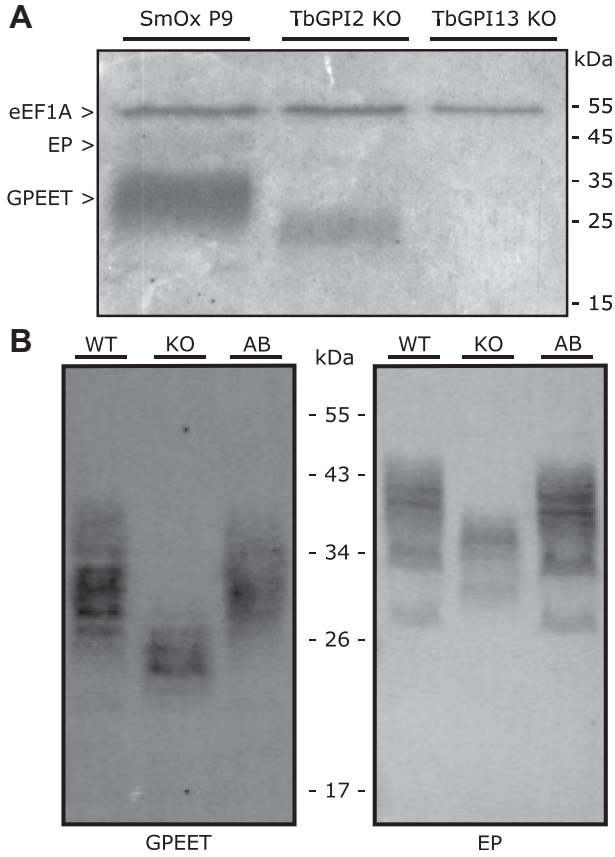

Figure 3. Analyses of GPEET and EP procyclin in TbGPI2-KO cells. *A*, *Trypanosoma brucei* SmOx P9, TbGPI2-KO, and TbGPI13-KO parasites were grown for 16 h in the presence of [^{3}H]-ethanolamine. Proteins were analyzed by SDS-PAGE followed by fluorography. *B*, *T. brucei* SmOx P9 (WT), TbGPI2-KO (KO), and TbGPI2-KO/HA (AB) parasites were cultured under standard conditions, and proteins were analyzed by SDS-PAGE followed by immunoblotting using α-GPEET 5H3 (*left panel*) or α-EP247 (*right panel*) antibodies. Molecular mass markers are indicated in the margins.

factor 1a (48)—the appearance of this band serves as a control for [^{3}H]-ethanolamine labeling in our experiments.

To extend the results of our radiolabeling experiments, we probed for GPEET and EP in TbGPI2-KO parasites by immunoblotting using specific antibodies. The results show that TbGPI2-KO cells express both GPEET and EP (Fig. 3*B*) and that both procyclins had distinctly lower apparent masses in TbGPI2-KO than parental parasites. Again, the expression of HA-TbGPI2 in the TbGPI2-KO background completely restored the parental phenotypes (Fig. 3*B*). A similar reduction in apparent molecular mass for EP procyclin was also observed when TbGPI2 was knocked out in a *T. brucei* 427–derived CRISPR-competent background (Fig. S3).

Previous studies showed that disruption of the GPI biosynthesis pathway may lead to retention and accumulation of normally GPI-anchored procyclins inside the cell (49). Although TbGPI2-KO cells retain the ability to synthesize GPI-anchored procyclins as shown above, we considered whether these proteins are indeed trafficked to the cell surface. Using immunofluorescence microscopy, we found a typical surface staining pattern for both EP and GPEET procyclin in TbGPI2-KO parasites that was indistinguishable from that of parental cells (Fig. 4*A*). Analysis by flow cytometry revealed a slight decrease in surface-localized EP and GPEET procyclins (Fig. 4*B*). The parental phenotype was completely restored on expressing HA-tagged TbGPI2 in TbGPI2-KO parasites (Fig. 4*B*). Thus, TbGPI2-KO cells synthesize non-native, GPI-anchored procyclins of a lower molecular weight that nonetheless are trafficked to the cell surface.

GPI anchors in TbGPI2-KO parasites are underglycosylated

We hypothesized that the non-native procyclin structures seen in TbGPI2-KO cells are due to underglycosylation of the GPI anchor. To investigate this, we purified procyclins from parental, TbGPI2-KO mutant and TbGPI2-KO mutants expressing TbGPI2-HA (add-back cells) and analyzed them as described in Scheme S1. This process involves subjecting the procyclins to aqueous hydrofluoric acid dephosphorylation, a process that liberates GPI anchor glycans from the procyclin polypeptide and lysophosphatidic acid lipid components of the PI moiety. The released GPI glycans are subsequently permethylated, a procedure that removes the fatty acid from the inositol ring and methylates all free hydroxyl groups and converts the amine group of the GlcN residue to a positively charged trimethyl quaternary ammonium ion (49). When infused into a mass spectrometer in the presence of sodium acetate, the permethylated GPI glycans appear in the MS1 spectra as triply charged $[M+2Na]^{3+}$ precursor ions. On subsequent fragmentation by collision-induced dissociation (CID), the triply charged precursor ions generate intense doubly charged product ions in the MS2 spectra because of the elimination of the inositol

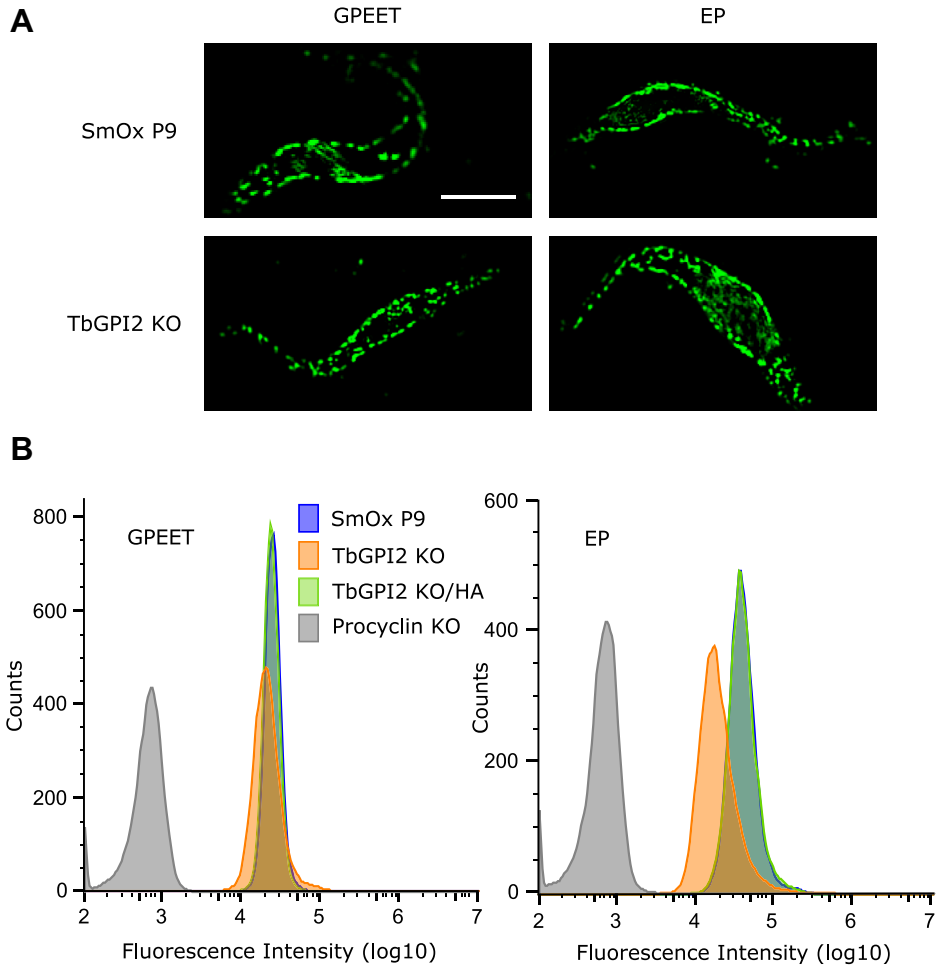

Figure 4. Surface localization of EP and GPEET procyclins. *A*, *Trypanosoma brucei* SmOx P9 (*top panels*) and TbGPI2-KO (*bottom panels*) parasites were fixed with paraformaldehyde, and procyclins were visualized by fluorescence microscopy using α-GPEET 5H3 (*left panels*) or α-EP247 (*right panels*) antibodies in combination with the corresponding fluorescent secondary antibodies. The scale bar represents 5 μm. *B*, *T. brucei* SmOx P9 (*blue*), TbGPI2-KO (*orange*), and TbGPI2-KO/HA (TbGPI2-KO parasites expressing HA-tagged TbGPI2; *green*) parasites were labeled as in panel *A*, and surface labeling of GPEET and EP was quantified by flow cytometry. *T. brucei* procyclin null parasites (Procyclin KO; (43)) were used as a negative control.

residue and the quaternary amine group (Scheme S1). Further CID fragmentation of these doubly charged product ions yields structurally informative MS3 spectra (Scheme S1). Glycan structure assignments are made by correlating the *m/z* values of the permethylated GPI glycan precursor ions, and their respective product ions in MS2 and MS3, with their theoretical and previously reported values (7, 8, 49).

The TbGPI2-KO mutant sample contained a series of triply charged $[M+2Na]^{3+}$ precursor ions in MS^1 (Fig. S4, *A* and *B*) consistent with GPI glycans with different numbers of Hex-HexNAc repeats and with and without sialic acid residues (Table S1) (7, 8). The same ions were observed in the samples from the parental and add-back cell lines.

The identities of triply charged $[M+2Na]^{3+}$ GPI glycan ions were proposed from MS^1, MS^2, and MS^3 data. For example, the $[M+2Na]^{3+}$ ions at *m/z* 888.45 in the MS^1 spectra are consistent with permethylated GPI glycans of composition $(Gal_5GlcNAc_2)Man_3GlcN(Me_3)^+Ino$ in the parental, add-back, and TbGPI2-KO samples (Table S1). In all three cases, doubly charged $[M+2Na]^{2+}$ fragment ions at *m/z* 1186.56 were generated in the MS^2 spectra by CID fragmentation of the *m/z* 888.45 $[M+2Na]^{3+}$ precursor ions (Fig. S5). Further CID fragmentation of the $[M+2Na]^{2+}$ fragment ions at *m/z* 1186.56 produced similar MS^3 spectra for all three samples that can be assigned to a known GPI-glycan structure (Fig. 5). The smallest and largest GPI glycans observed were $(Gal_5GlcNAc_2)Man_3GlcN\text{-}Ino$ and $(Gal_{11}GlcNAc_8SA_1)Man_3GlcN\text{-}Ino$, respectively (Table S1).

Interestingly, the triply charged GPI glycan ions were more intense in the MS^1 spectrum of the TbGPI2-KO mutant sample than in the parental and TbGPI2-KO/HA add-back samples. This is consistent with the TbGPI2-KO mutant GPI glycans being smaller than those of the WT and TbGPI2-KO/HA add back, as the larger molecular species are harder to ionize and observe in MS^1. Our results suggest, therefore, that the ∼10-kDa lower molecular weight of GPEET seen in SDS-PAGE fluorograms of $[^3H]$-ethanolamine-labeled cells is due to a reduction in the number of LacNAc and/or lacto-N-biose repeats (Fig. 3*A*).

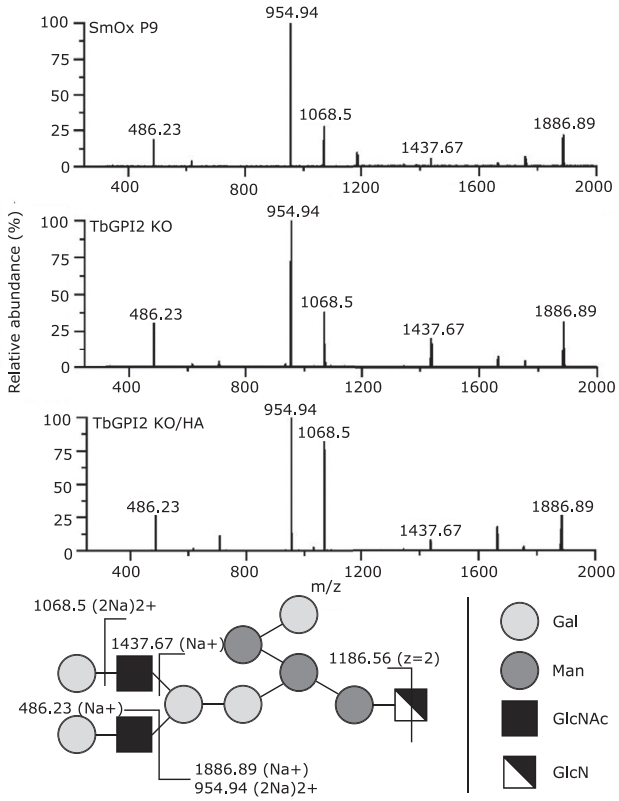

Figure 5. MS^3 product ion spectra of permethylated GPI glycans in TbGPI2-KO and control parasites. Permethylated GPI glycans from parental (*top*), TbGPI2-KO (*middle*), and TbGPI2-KO/HA (*bottom*) mutant parasites were analyzed by positive-ion ES-MS. Triply charged $[M + 2Na]^{3+}$ ions observed at *m/z* 888.45 for each sample were fragmented (MS^2), generating a doubly charged product ion at *m/z* 1186.56 (Fig. S5). This ion was further fragmented (MS^3) to generate the product ion spectra shown. Assignments of the major product ions are indicated on the *inset* diagram. GPI, glycosylphosphatidylinositol.

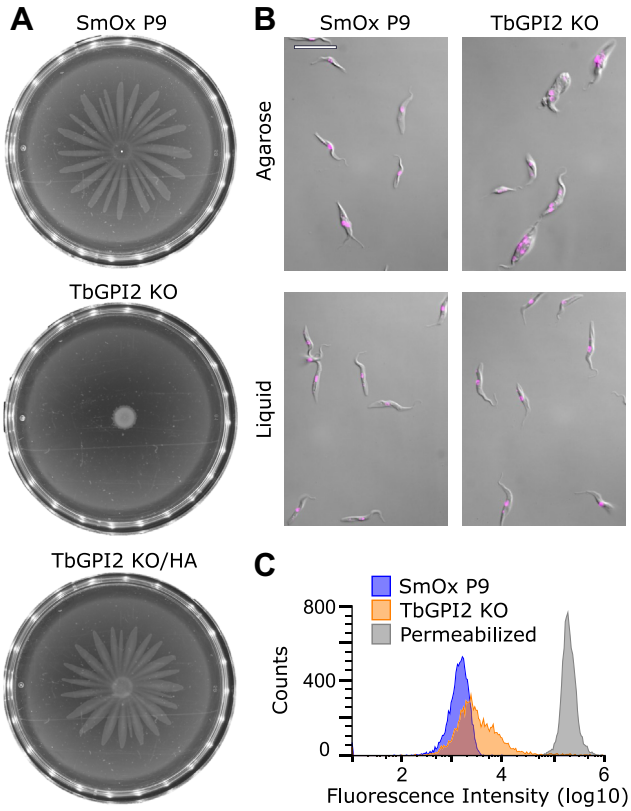

Figure 6. Behavior of TbGPI2-KO trypanosomes grown on agarose plates. *A*, *Trypanosoma brucei* SmOx P9 (*top*), TbGPI2-KO (*middle*), and TbGPI2-KO/HA (*bottom*) parasites were inoculated on agarose plates. The plates were photographed after 4 days of incubation at 27 °C. *B*, parasites grown on agarose plates for 2 days and subsequently washed off (*top*) or in liquid culture for 2 days (*bottom*) were stained with Hoechst dye and examined by light microscopy. The scale bar represents 20 μm. *C*, parasites grown as in panel *A* were stained with propidium iodide and subjected to flow cytometry analysis.

TbGPI2 depletion leads to defects in social motility and growth on semisolid surfaces

We previously showed that a *T. brucei* mutant with a perturbation in *N*-linked glycosylation and GPI glycosylation (50) was impaired in its ability to perform social motility (SoMo), a form of collective migration on agarose plates, as well as to colonize the tsetse fly vector (51). We therefore examined the effect of the TbGPI2 deletion on SoMo. Our results reveal that TbGPI2-KO cells showed essentially no SoMo (Fig. 6*A*) and that the parental phenotype could be restored by expressing TbGPI2-HA (Fig. 6*A*). In addition, we noticed morphological abnormalities (Fig. 6*B*, upper panels) and decreased viability (Fig. 6*C*) of TbGPI2-KO parasites cultivated on agar plates compared with parental cells (Fig. 6*B*, upper panels). Approximately one of four TbGPI2-KO parasites retrieved from SoMo plates contained multiple nuclei and appeared enlarged and dysmorphic compared with parental cells. In liquid culture, morphological abnormalities were only observed in a small fraction of cells (<5%). In addition, a similar defect in SoMo was also seen in *T. brucei* 427-derived TbGPI2-KO parasites (Fig. S3).

Previous work indicated that procyclin null mutants are capable of SoMo (52); as these mutants compensated for the lack of procyclins by expressing free GPIs on their surfaces (43, 53), it appeared likely that the GPI moieties themselves might be sufficient for SoMo. This observation is consistent with our findings that mutants lacking TbRft1 (50) and TbGPI2 (this study) produce truncated GPI anchors and have fewer free GPIs. Thus, the GPIs in these mutants are inadequate in terms of supporting SoMo despite the cells having normal levels of surface procyclins.

There are several parallels between SoMo and the swarming motility of bacteria on semisolid surfaces. Cells face a number of challenges: they need to extract water from the surface to remain hydrated, and they must overcome friction and surface tension to move. Bacteria accomplish this by producing (lipo) polysaccharides and surfactants such as glycolipids or lipidated peptides (54–57). It is conceivable that GPIs act as lubricants facilitating movement and that the glycocalyx of GPI-anchored proteins or free GPIs protects cells against dehydration.

The GPI GlcNAc transferase complex is affected by the absence of TbGPI2

To study the effects of the absence of TbGPI2 on the GPI GlcNAc transferase complex, we selected TbGPI1, another

multispanning membrane protein subunit of the complex, as a reporter. We epitope-tagged TbGPI1 in *T. brucei* SmOx P9 and TbGPI2-KO parasites at its genomic locus and compared its expression level and inclusion in the GPI GlcNAc transferase complex in the two cell lines. Analysis by SDS-PAGE and immunoblotting showed that expression of cMyc-tagged TbGPI1 is unaffected by the absence of TbGPI2 (Fig. 7*A*). Native PAGE revealed that TbGPI1 from SmOx P9 parasites migrates as a broad band between the 242-kDa and 720-kDa molecular mass markers (Fig. 7*B*), reflecting its association with the GPI GlcNAc transferase complex. In a previous report (39), a GPI GlcNAc transferase complex isolated from *T. brucei* bloodstream by pull-down of cMyc-tagged TbGPI3 was seen to run closer to the 242-kDa marker. The reason for the difference on native PAGE between our data and the published report is not clear but could be due to heterogeneity of the complexes revealed by using different baits for pull-down (TbGPI3 *versus* TbGPI1) or differences in the architecture of the complexes in bloodstream *versus* procyclic trypanosomes. Despite its comparable expression level in parental SmOx P9 and TbGPI2-KO cells, TbGPI1 was detected at a much lower level in native PAGE analysis of extracts from the TbGPI2-KO parasites (Fig. 7*B*) and appeared at the higher end of the molecular mass spectrum (480–720 kDa) seen for native GPI GlcNAc transferase. This result suggests that in the absence of TbGPI2, TbGPI1 is poorly recruited into the GPI GlcNAc transferase complex and that complexes that do retain TbGPI1 run at a higher apparent molecular mass.

TbGPI2 partially localizes to the Golgi apparatus

The phenotypic profile of TbGPI2-KO cells is reminiscent of some features of TbRft1-KO trypanosomes, specifically GPI underglycosylation (50) and SoMo defects (51). Immunofluorescence microscopy revealed that TbRft1 was localized to both the ER and the Golgi apparatus, hinting at a possible explanation for its role in regulating Golgi-localized GPI glycosylation (50). Because of the link between TbGPI2 and GPI glycosylation, we considered that TbGPI2 may also be localized to both the ER and Golgi apparatus.

Subcellular localization of TbGPI2 was investigated in both the isogenic parental strain (SmOx P9) expressing *in situ* HA-tagged TbGPI2 (TbGPI2-HA(is)) and the add-back cell line expressing TbGPI2-HA in the TbGPI2-KO background used in the above experiments. Analysis of TbGPI2-HA levels by SDS-PAGE and immunoblotting showed that the TbGPI2-HA(is) is expressed approximately 100-fold less than the ectopic copy of TbGPI2-HA (Fig. 8*A*). Examination of these parasites by immunofluorescence microscopy showed extensive colocalization of TbGPI2-HA(is) with the ER resident chaperone TbBiP (Fig. 8*B*), indicating that TbGPI2 localizes to the ER as expected. In addition, in >62% of parasites (n = 133), TbGPI2-HA(is) was found to also colocalize with TbGRASP (Fig. 8*C*), a Golgi-resident protein (58). Similar results were also obtained for TbGPI2-HA ectopically expressed in TbGPI2-KO parasites, with >67% of parasites (n = 122) showing colocalization of TbGPI2 and TbGRASP (Fig. S6). We previously showed that (i) these levels of colocalization with a Golgi marker are highly significant and not a random occurrence, as colocalization is detected in fewer than 35% of cells expressing an epitope-tagged version of the ER resident protein TbEMC3 (Tb927.10.4760) (50) and (ii) it is unlikely to be a result of saturation of the retention system for ER resident proteins because overexpression of TbEPT, another ER-localized membrane protein (59), did not result in Golgi localization (50). Together, these results suggest that whereas TbGPI2 is predominantly ER-localized, it also partially localizes to the Golgi apparatus.

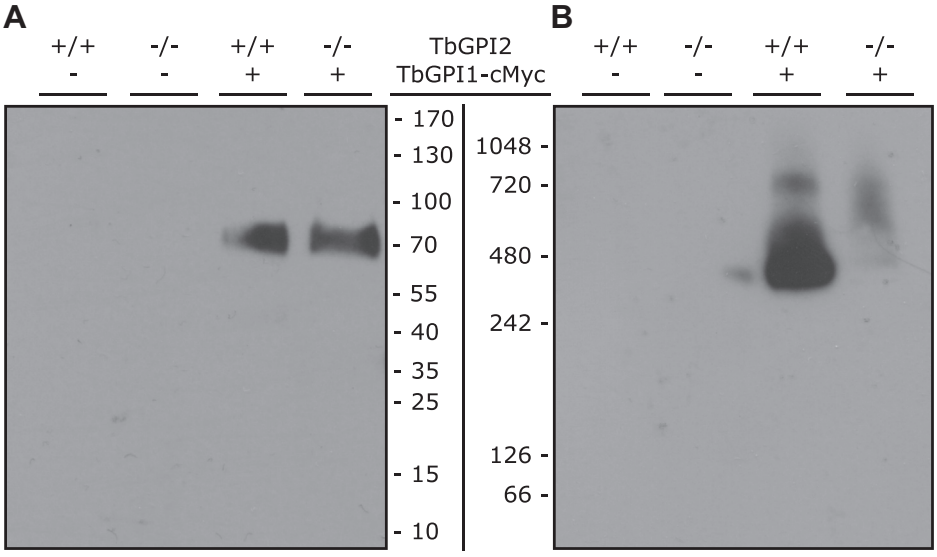

Figure 7. GlcNAc transferase complex in TbGPI2-KO trypanosomes. *Trypanosoma brucei* SmOx P9 (+/+) and TbGPI2-KO (–/–) parental parasites (–), and SmOx P9 (+/+) and TbGPI2-KO (–/–) parasites expressing cMyc-tagged TbGPI1 (+), were immunoprecipitated from cell extracts prepared under non-denaturing conditions and analyzed by SDS-PAGE (*A*) and native PAGE (*B*). TbGPI1 was detected by immunoblotting using the anti-cMyc antibody. The lanes contain identical cell equivalents. Molecular mass markers are indicated in kilodalton in the margins.

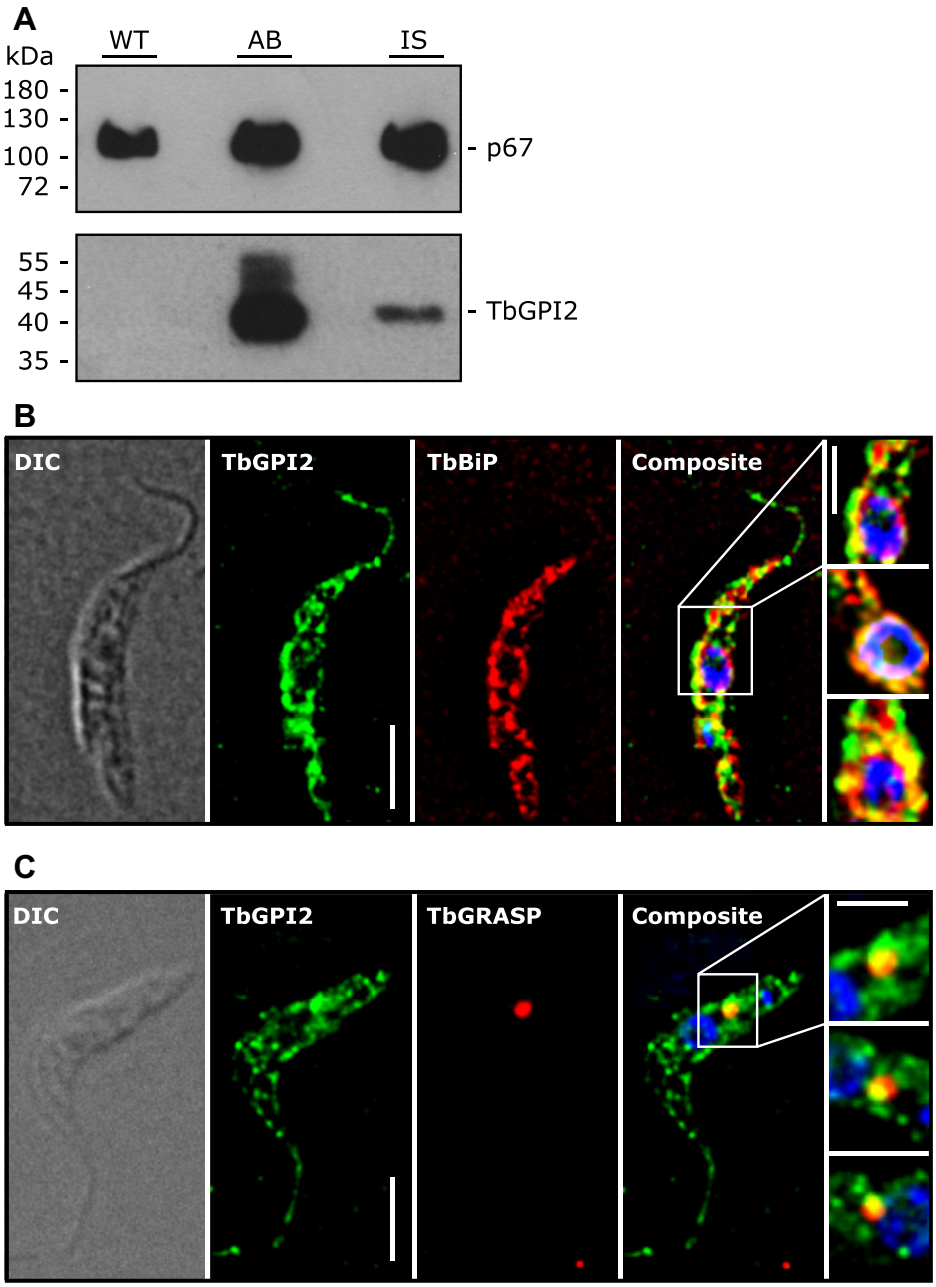

Figure 8. Subcellular localization of TbGPI2. *A*, proteins from parasites expressing TbGPI2-HA in the GPI2-KO background (add back [AB]) or *in situ*–tagged TbGPI2-HA(is) (IS) were analyzed by SDS-PAGE and immunoblotting using antibodies against HA and p67 (as the loading control). Equal cell equivalents were applied. *B* and *C*, parasites expressing *in situ*–tagged TbGPI2-HA(is) were fixed and stained with antibodies against HA (TbGPI2; *B* and *C*), TbBiP (*B*), and TbGRASP (*C*) and analyzed by immunofluorescence microscopy. DNA in the composites was stained with DAPI (*blue*). Colocalization of TbGPI2 and TbBiP/TbGRASP in the composites is represented in *yellow*. Images represent single slices from an image stack. Areas of interest are shown in the enlargements on the *right*. The scale bar represents 10 μm, and the scale bar in the enlargements represents 5 μm.

Concluding remarks

Gpi2/PIG-C is an essential component of the GPI GlcNAc transferase complex in yeast (11, 23) and human (17) cells, but its precise function is not known. We now report that TbGPI2 is important but not essential for *T. brucei* GPI GlcNAc transferase activity, which persists in TbGPI2-KO parasites at a low level as seen by *in vitro* assays and metabolic labeling experiments. The residual GPI GlcNAc transferase activity produces sufficient GPIs for procyclin anchoring, albeit at the expense of free GPIs. A low level of GPI-GlcNAc transferase activity has also been reported to persist in mammalian cells lacking GPI1 (60). Furthermore, we show that in the absence of TbGPI2, the architecture of the GPI GlcNAc transferase complex is compromised, losing most of its content of TbGPI1. This disruption suggests a central scaffolding role for TbGPI2 in recruiting/organizing other subunits of the complex, different from the organization of the yeast and mammalian complex (61), where Gpi1 was proposed to link Gpi3 and other subunits to Gpi2. Together, these results

indicate that in the absence of TbGPI2, both the architecture and the activity of the *T. brucei* GPI GlcNAc transferase are heavily compromised. More work needs to be done to sort out the arrangement and stoichiometry of the various subunits in the complex to understand their individual roles.

TbGPI2-KO trypanosomes are able to synthesize GPI-anchored proteins, but their GPI anchors are under-glycosylated, which may underly their inability to perform SoMo. GPI anchors are sialylated in the Golgi apparatus by *trans*-sialidase, which itself is a GPI-anchored protein (36, 62). Our results show that elimination of TbGPI2 leads to a decreased surface localization of EP procyclin, but normal levels of GPEET procyclin. Despite these near-normal levels of procyclins, we cannot exclude that the levels of *trans*-sialidase may also be decreased in TbGPI2-KO parasites, which in turn may result in undermodification of the procyclin GPI anchors as reflected by their lower molecular masses.

As GPI glycosylation largely occurs in the Golgi apparatus (7, 8), it is possible that the Golgi pool of TbGPI2 that we observe may directly or indirectly influence the extent to which GPI side chains are extended. Perhaps TbGPI2 interacts with the enzymes responsible for GPI glycosylation, thereby affecting their function. This possibility could be tested in future studies aimed at detecting physical or genetic interaction partners of TbGPI2.

Finally, in *Candida albicans*, GPI2 has been proposed to play an additional role in ergosterol biosynthesis through indirect interaction with CaERG11 *via* CaGPI19 (63) as well as Ras1 signaling (23). Thus, a moonlighting function of TbGPI2 in the GPI glycosylation can be envisioned.

Experimental procedures

Unless otherwise stated, reagents were purchased from Merck KGaA. Restriction enzymes were from Thermo Fisher Scientific. Tritium-labeled compounds were from American Radiolabeled Chemicals Inc and PCR reagents and restriction enzymes from Promega Corporation. Acrylamide mix was from National Diagnostics.

Trypanosome cultures

T. brucei SmOx P9 pTB011 procyclic forms (64) (henceforward termed SmOx P9) were maintained at 27 °C in SDM79 containing 10% (v/v) heat-inactivated fetal bovine serum, 160 μM hemin, 90 μM folic acid, 2 μg/ml puromycin, and 5 μg/ml blasticidin. TbGPI2-KO, TbGPI2-KO/HA, and *in situ*–tagged parasites were grown under the same conditions with additional selection antibiotics added (for TbGPI2-KO: 25 μg/ml hygromycin, 1 μg/ml G418; for TbGPI2-KO/HA: 25 μg/ml hygromycin, 1 μg/ml G418, 3.6 μg/ml phleomycin; for *in situ*: 3.6 μg/ml phleomycin).

Generation of T. brucei *TbGPI2-KO parasites*

TbGPI2-KO parasites were generated using CRISPR/Cas9 technique as described before (64). In addition, TbGPI2-KO parasites were also generated in a *T. brucei* 427–derived CRISPR-competent background (65). Briefly, two resistance gene cassettes were generated by PCR using primers 1 and 2 (Table S2) and template plasmid pPOTv6 (66) containing resistance genes for hygromycin and neomycin, respectively. The cassettes were flanked with homology sequences of 30 nt to replace both alleles of the target gene *via* homologous recombination. Two single-guide RNA templates containing a T7 polymerase promoter, a Cas9-binding site, and a 20-nt targeting sequence were generated by PCR using primer pairs 3/5 and 4/5 (Table S2), respectively. All PCRs were performed using the Expand High Fidelity PCR System (Roche Diagnostics GmbH), and primers were designed using the online tool at www.leishgedit.net. All PCR products were pooled and purified using the Wizard SV Gel and PCR Clean-Up System (Promega). DNA (10 μg) was transfected into SmOx P9 cells using a 4D-Nucleofector System (Lonza Group AG) with program FI-115. After 24 h, selection antibiotics were added, and the culture was diluted 1:25 and distributed into 24-well plates. TbGPI2 gene KO was verified by PCR using extracted gDNA from KO clones and primer pairs 6/7, 6/8, 6/9, and 6/10 (Table S2), as well as by Northern and Southern blotting (see below).

Generation of T. brucei *TbGPI2 add-back parasites*

TbGPI2 ORF was amplified from SmOx P9 gDNA using primer pairs 11/12 and 11/13 (Table S2), yielding untagged and HA-tagged constructs of TbGPI2 flanked by *Hind*III and *Xho*I restriction sites, which were then cloned into plasmid pMS1720RNAiBSF (67). Plasmids (10 μg) were then linearized with *Not*I and transfected into SmOx P9 TbGPI2-KO cells using a 4D-Nucleofector System (Lonza Group AG) with program FI-115. After 24 h, the selection antibiotic was added, and the culture was diluted 1:250 and distributed into 24-well plates. TbGPI2 gene add back was verified by PCR using extracted gDNA from add-back clones and the following primer pairs: 6/7, 11/12 (Table S2). Protein expression was analyzed by SDS-PAGE followed by immunoblotting against the HA epitope.

Northern and Southern blotting

TbGPI2 mRNA expression was assayed by Northern blotting as described before (44). Genomic DNA was isolated and digested with *Bgl*II or *Cla*I followed by Southern blotting as previously described (44). A radioactively labeled probe corresponding to the coding region of TbGPI2 was generated using a Megaprime DNA-labeling system (GE Healthcare) according to the manufacturer's instructions. Signals were detected by exposure of the blots to a Phosphorimager screen (Amersham Biosciences) followed by scanning with a Typhoon FLA 7000 (GE Healthcare).

In situ *tagging of TbGPI1 and TbGPI2*

TbGPI1 and TbGPI2 were *in situ* tagged in SmOx P9 and, in the case of TbGPI1, in TbGPI2-KO cells using CRISPR/Cas9 technique as described above. Briefly, the resistance gene cassettes were generated by PCR using primer pairs 14/15 (TbGPI1) and 17/18 (TbGPI2) as described above. The

cassettes consisted of a cMyc (TbGPI1) or HA (TbGPI2) tag sequence and a phleomycin (TbGPI1) or hygromycin (TbGPI2) resistance gene and were flanked by homology sequences of 30 nt to insert between the last codon and the stop codon of the respective gene by homologous recombination. A single-guide RNA template was generated by PCR using primer pairs 5/16 (TbGPI1) or 5/19 (TbGPI2) as described above. Ten microgram of pooled and purified PCR was transfected into the cells as described above. Twenty-four hours after transfection, the selection antibiotic was added, and the cultures were diluted 1:100 (for SmOx P9) and 1:3 (for TbGPI2-KO) and distributed into 24-well plates. Protein expression was analyzed by SDS-PAGE followed by immunoblotting against the cMyc or HA epitope, respectively.

[^{3}H]-ethanolamine labeling of GPI precursors and GPI-anchored proteins

GPI precursors and GPI-anchored proteins were labeled and extracted as previously described (45). Briefly, 5×10^8 trypanosomes were cultured for 16 to 18 h in the presence of 50 μCi of [^{3}H]-ethanolamine. The cells were harvested by centrifugation and washed twice with Tris-buffered saline (140 mM NaCl, 10 mM Tris, pH 7.4). Subsequently, phospholipids were extracted twice with chloroform/methanol 2:1 (v/v; CM fraction). GPI precursors and free GPIs (43, 68) were extracted three times with chloroform/methanol/water 10:10:3 (v/v/v; CMW fraction), and GPI-anchored proteins were extracted twice with 9% butan-1-ol in water (v/v; BuOH fraction). The CMW fractions were further partitioned between butan-1-ol and water, yielding fractions CMW_{but} and CMW_{aq} containing GPI precursors and free GPIs, respectively. All fractions were pooled and dried, and aliquots were used for liquid scintillation counting.

TLC

CMW_{but} or butanol extracts containing GPI precursors were resolved by TLC using Silica Gel 60 plates and chloroform/methanol/water (10:10:3; v/v/v) as the solvent system. The chromatograms were visualized using a Raytest Rita* radioactivity TLC analyzer (Berthold Technologies).

Protein analysis

CMW_{aq} and BuOH extracts were subjected to SDS-PAGE under reducing conditions (69). Briefly, samples were dried and resuspended in 1× loading buffer (15% (v/v) glycerol, 5% (v/v) β-mercaptoethanol, 2.5% (w/v) SDS, 50 mM Tris, 1 mM EDTA, 0.0025% (w/v) bromophenol blue) and separated using 12% polyacrylamide gels, containing 0.1% (w/v) SDS, at constant 120 V. Gels were soaked in Amplify (GE Healthcare), dried, and exposed to films (Carestream Health Medical X-ray Blue) at −70 °C. HA-tagged TbGPI2 and cMyc-tagged TbGPI1 were analyzed by immunoblotting as described before (50). EP and GPEET procyclins were analyzed by immunoblotting using the LI-COR detection system (Odyssey Infrared Imager model 9120, Odyssey Application Software, version 3.0.30). Primary antibodies were mouse α-GPEET 5H3 (70) at dilution 1:2500 and mouse α-EP247 at dilution 1:2500, and the secondary antibody was goat α-mouse IRDye 800CW at dilution 1:10,000.

Immunofluorescence microscopy

Approximately 2.5×10^6 trypanosomes were harvested by centrifugation, washed with cold PBS (137 mM NaCl, 2.7 mM KCl, 10 mM Na_2HPO_4, and 1.76 mM KH_2PO_4, pH 7.4), resuspended in a small volume of PBS, spread on a microscopy slide, and left to adhere for 20 min. Subsequently, parasites were fixed using 4% (w/v) paraformaldehyde in PBS for 10 min. After three washes for 5 min with cold PBS, cells were permeabilized in 0.2% (w/v) Triton X-100 for 20 min. After three additional washes and incubation in the blocking solution (2% (w/v) bovine serum albumin in PBS) for 30 min, the blot was incubated with the primary antibody in the blocking solution for 45 min at room temperature. Antibodies used were mouse α-GPEET 5H3 (70), mouse α-EP247 (clone TRBP1/247, Cedarlane) and mouse anti-HA (clone 16B12, Enzo Life Sciences) at dilutions of 1:500, and rabbit anti BiP (kindly provided by J.D. Bangs, University of Buffalo, Buffalo, NY) and rabbit anti-TbGRASP (kindly provided by G. Warren, Vienna Biocenter, Vienna, Austria) at concentrations of 1:2500 and 1:1500, respectively. After washing, the cells were incubated for 45 min with Alexa Fluor 488– or Alexa Fluor 594–conjugated goat α-mouse or goat α-rabbit secondary antibodies at 1:1000 dilutions in the blocking buffer. After washing, the cells were mounted with VECTASHIELD DAPI (Vector Laboratories). Immunofluorescence image stacks were captured on a Leica SP2 using a 100× oil objective. Image stacks were 3D deconvolved with the Leica LAS AF Version 2.1.0 software (Leica Microsystems CMS GmbH), and single slices of the stacks were used to analyze subcellular colocalization.

Flow cytometry

Flow cytometry was performed on live trypanosomes. Antibodies were diluted in the corresponding incubation medium. Primary antibodies used were mouse α-GPEET 5H3 (70) at a dilution of 1:1000, or mouse α-EP247 at 1:500. Parasites (4×10^6 cells) were harvested by centrifugation. All subsequent steps were performed at 4 °C. The cells were resuspended in 200-μl medium containing the primary antibody and incubated with rotation for 30 min. After addition of 800-μl medium, cells were pelleted and washed once with 800-μl medium. After pelleting, the cells were resuspended, incubated with Alexa Fluor 488–conjugated secondary antibodies (Invitrogen, and Thermo Fisher Scientific) at dilutions of 1:1000, and washed as described for the primary antibody. After resuspension in 1.6 ml medium, fluorescence of labeled and unstained control cells was quantified with an ACEA NovoCyte benchtop flow cytometer (Agilent Technologies). After applying a cut-off of 7.5×10^5 to the forward scatter, a total of 1×10^4 events were recorded and analyzed using FlowJo software (BD Life Sciences) without gating.

SoMo

Trypanosomes were cultured in the liquid medium or on semisolid agarose in a humidified incubator at 27 °C and 2.5% CO_2. Cells in liquid culture were maintained between 1×10^6 and 1.5×10^7 cells ml^{-1} by daily monitoring and diluted into the same culture flask (TPP vent screw cap). Semisolid culture plates containing 0.4% (w/v) agarose/medium in a 90-mm-diameter petri dish for SoMo assays were prepared as previously described (52). Directly after air-drying for 1 h, the surface of SoMo plates was inoculated with 2×10^5 cells (5-µl liquid culture concentrated to 4×10^7 cells). Five to Ten minutes after inoculation and without sealing the plates with Parafilm, plates were transferred to the humidified incubator. The growth pattern of trypanosome communities was documented daily with a digital camera in a dark room with LED white-light illumination from below.

Analysis of trypanosomes cultured on SoMo plates by microscopy and propidium iodide staining

Trypanosomes were cultured on SoMo plates as described in the section "SoMo". Cellular morphology and uptake of propidium iodide were assessed for cells grown in the liquid culture or taken off SoMo plates. Samples were prepared individually and analyzed immediately to avoid artefactual effects caused by prolonged exposure to treatments. For staining with propidium iodide, cells were taken off a SoMo plate by two washes with 1× PBS, and 300 µl of an appropriate dilution was supplemented with propidium iodide (1.0 mg/ml stock solution) to a final concentration of 5 µg/ml. Two different plates per cell line and time point were analyzed. For reference, cells from the liquid culture were washed twice with 1× PBS and analyzed live or after fixation (1 h in 70% ethanol on ice (71)), with and without 5 µg/ml propidium iodide. Staining with propidium iodide was quantified with a benchtop flow cytometer as described in the section "Flow cytometry", but a cut-off of 5×10^5 was applied to the forward scatter. For morphological analysis by microscopy, trypanosomes were taken off a SoMo plate 2 days after inoculation. Cells were removed from three spots by careful pipetting with 10-µl growth medium per spot. Pooled cells were paralyzed by mixing 3:2 with 10% sodium azide and immediately mounted with approximately 1.5 volumes Mowiol containing 10 µg/ml Hoechst DNA stain (final concentration of approximately 1.5% sodium azide). For reference, cells from the liquid culture were concentrated by centrifugation, and 3 µl ($\sim 1.5 \times 10^5$ cells) was paralyzed and mounted as described. Microscopy images were acquired over a period of 15 to 30 min after mounting. Differential interference contrast and epifluorescence microscopy were performed with a Leica DM5500 instrument equipped with a DFC350 FX monochrome CCD camera using 100× objective (HC PL APO 100X/1.40 OIL PH3 CS). Images were processed with ImageJ version 2.0.0 (Fiji).

Cell-free labeling of GPI precursors with UDP-[^{3}H]GlcNAc

Cell-free labeling was performed as previously described (30, 33). Briefly, 2.5×10^8 trypanosomes were harvested by centrifugation, washed twice with PBS, and hypotonically lysed on ice for 5 min in 250-µl lysis buffer (0.1 mM TLCK, 1 µg/ml leupeptin). The cell lysate was added to 250-µl HKMTLG buffer (100 mM Hepes, 50 mM KCl, 10 mM $MgCl_2$, 0.1 mM TLCK, 1 µg/ml leupeptin, 20% glycerol, pH 7.4), snap-frozen, and stored at −80 °C for at least 24 h.

Before use, cell lysates were thawed, washed twice with 1-ml ice-cold HKMTL buffer (100 mM Hepes, 50 mM KCl, 10 mM $MgCl_2$, 0.1 mM TLCK, 1 µg/ml leupeptin, pH 7.4), resuspended in 150 µl 2× HKMTL buffer containing 10 mM $MnCl_2$ and 0.2 µg/ml tunicamycin, and prewarmed to 27 °C. For each sample, 1 µl (equal to 1 µCi) UDP-[^{3}H]GlcNAc was added to 30-µl prewarmed DA buffer (2 mM DTT, 2 mM ATP). Thirty microliter of the cell lysate was added, and the mixture was incubated at 27 °C for the indicated time. The assay was terminated by addition of 400-µl chloroform/methanol 1:1 (v/v) for a final chloroform/methanol/water ratio of 10:10:3 (v/v/v). GPI precursors were solubilized by water bath sonication and incubation on ice. Insoluble compounds were removed by centrifugation. The pellet was re-extracted with 250-µl chloroform/methanol/water 10:10:3 (v/v/v). The extracts were pooled, dried under N_2, and purified by partitioning between n-butanol and water. The upper (organic) phase was collected, while the lower phase was re-extracted with water-saturated butanol, both organic phases were pooled, and remaining impurities were removed by back extraction with butanol-saturated water. The purified organic phases were subjected to β-counting and TLC analysis as described above.

Mass spectrometry analysis of procyclin-derived GPI anchors

Extraction and purification of procyclins. Procyclins (both GPEET and EP forms) were purified from 10^{10} cells by organic solvent extraction and octyl-Sepharose chromatography as previously described (27, 28) but with a slight modification. Briefly, the cells were extracted three times with chloroform/methanol/water (10:10:3, v/v). After the delipidation process, the pellet was dried under N_2 and subsequently extracted twice with 9% butan-1-ol in water. The supernatant of 9% butan-1-ol extracts were pooled and dried under N_2. To further purify the extracted procyclins, the dried samples were redissolved in 1 ml of buffer A (5% propan-1-ol in 0.1 M ammonium acetate) and applied to 0.5 ml of octyl-Sepharose 4B packed in a disposable column and pre-equilibrated with buffer A. The column was washed with 3 ml of buffer A followed by 3 ml of buffer B (5% propan-1-ol). The procyclins were eluted in 2.5 ml of buffer C (50% propan-1-ol) and concentrated and dried by rotary evaporation.

Permethylation and ES-MS of GPI glycans. The dried procyclin samples were treated with 100 µl of ice-cold 50% aqueous hydrogen fluoride for 24 h at 0 °C to cleave the GPI anchor ethanolamine-phosphate-mannose and inositol-phosphate-acylglycerol phosphodiester bonds. The samples were freeze-dried to evaporate the remaining aqueous hydrogen fluoride and redissolved in 100-µl water and centrifuged at 16,000*g* for 10 min. The supernatant containing the GPI glycans was taken

for permethylation by the sodium hydroxide method, as described (7, 8). The permethylated GPI glycans, bearing a fixed positive charge in the form of an *N*-trimethyl-glucosamine quaternary ammonium ion, were dissolved in 100 µl of 80% acetonitrile, and 10% aliquots were dried and recovered in 10 µl of 80% acetonitrile and 0.5 mM sodium acetate. The samples were infused into the Orbitrap Fusion tribrid mass spectrometer (Thermo Scientific) using static infusion nanoflow probe tips (M956232AD1-S, Waters). Data were collected in the positive-ion mode for ES-MS, ES-MS^2, and ES-MS^3. Positive-ion spray voltage was 0.7 kV, and the ion transfer tube temperature was 275 °C. CID was used for MS^2 and MS^3 fragmentation, using 25 to 35% collision energy.

Protein analysis by native PAGE

The GPI GlcNAc transferase complex was immunoprecipitated from parasites expressing myc-tagged TbGPI1 as previously described (39). Briefly, 2 × 10^8 trypanosomes were harvested by centrifugation, washed twice with PBS, and lysed for 30 min on ice in 500-µl lysis buffer (50 mM Tris-HCl, 150 mM NaCl, 1% digitonin, pH 7.4). Insoluble components were removed by centrifugation at 16,000*g* for 20 min at 4 °C. The supernatant was incubated with α-cMyc agarose beads (Takara Bio) on a rotary wheel for 16 h at 4 °C. Bound complexes were eluted three times with 10-µl lysis buffer containing 0.5 mg/ml cMyc peptide. Eluted complexes were subjected to native PAGE as previously described (72). Briefly, the protein complexes were supplemented with 10× BN loading buffer (5% (w/v) Coomassie Brilliant Blue G-250, 500 mM 6-aminocaproic acid, 100 mM Bis-Tris·HCl, pH 7.0) and separated on a 4 to 15% polyacrylamide gel (Bio-Rad Laboratories). After separation, proteins were transferred on a polyvinylidene fluoride membrane and detected by immunoblotting against the cMyc epitope.

Data availability

The raw mass spectrometry data of parental, TbGPI2-KO/HA add back, and TbGPI2-KO glycan samples along with glycan interpretation and annotation can be accessed from GlycoPOST repository (Project ID: GPST000193.0) at https://glycopost.glycosmos.org/entry/GPST000193.0. All other data are contained within this article.

Supporting information—This article contains supporting information.

Acknowledgments—We thank Monika Rauch and Jennifer Jelk for technical assistance during parts of the study. A. J. thanks Sophie Stammherr for inspiring discussions. P. B. dedicates this article to Annina Niederer (1953–2021) for year-long support and encouragement.

Author contributions—A. J., M. A. J. F., and P. B. data curation; A. J., S. K., R. N., M. B., and P. B. formal analysis; A. J., R. N., M. B., M. A. J. F., I. R., A. K. M., and P. B. investigation; A. J., S. K., R. N., and M. B. visualization; A. J., S. K., R. N., and M. B. methodology; A. J. writing–original draft; R. H., M. A. J. F., I. R., A. K. M., and P. B. funding acquisition; R. H., A. K. M., and P. B. project administration; M. A. J. F., I. R., A. K. M., and P. B. supervision; M. A. J. F., I. R., A. K. M., and P. B. writing–review and editing; A. K. M. and P. B. conceptualization.

Funding and additional information—The work was supported by the Swiss National Science Foundation Sinergia grant CRSII5_170923 to R. H., A. K. M., and P. B., a Wellcome Trust Investigator Award (101842/Z13/Z) to M. A. J. F., and Swiss National Science Foundation grant 310030_184669 to I. R.

Conflict of interest—The authors declare that they have no conflicts of interest with the contents of this article.

Abbreviations—The abbreviations used are: Cas9, CRISPR-associated protein 9; CID, collision-induced dissociation; ER, endoplasmic reticulum; GlcN, glucosamine; GPI, glycosylphosphatidylinositol; PI, phosphatidylinositol; SoMo, social motility; TbGPI2-HA(is), *in situ* HA-tagged TbGPI2.

References

1. Orlean, P., and Menon, A. K. (2007) Thematic review series: Lipid posttranslational modifications. GPI anchoring of protein in yeast and mammalian cells, or: How we learned to stop worrying and love glycophospholipids. *J. Lipid Res.* **48**, 993–1011
2. Ferguson, M. A. J., Hart, G. W., and Kinoshita, T. (2015). In: Varki, A., Cummings, R., Esko, J., eds. *Glycosylphosphatidylinositol Anchors*, Academic Press, Cambridge, MA
3. Vidugiriene, J., and Menon, A. K. (1993) Early lipid intermediates in glycosyl-phosphatidylinositol anchor assembly are synthesized in the ER and located in the cytoplasmic leaflet of the ER membrane bilayer. *J. Cell Biol.* **121**, 987–996
4. Pottekat, A., and Menon, A. K. (2004) Subcellular localization and targeting of N -acetylglucosaminyl phosphatidylinositol de- N -acetylase, the second enzyme in the glycosylphosphatidylinositol biosynthetic pathway. *J. Biol. Chem.* **279**, 15743–15751
5. Vishwakarma, R. A., and Menon, A. K. (2005) Flip-flop of glycosylphosphatidylinositols (GPI's) across the ER. *Chem. Commun. (Camb.)*. https://doi.org/10.1039/b413196g
6. Sanyal, S., and Menon, A. K. (2009) Flipping lipids: Why an' what's the reason for? *ACS Chem. Biol.* **4**, 895–909
7. Izquierdo, L., Nakanishi, M., Mehlert, A., Machray, G., Barton, G. J., and Ferguson, M. A. J. (2009) Identification of a glycosylphosphatidylinositol anchor-modifying β1-3 N-acetylglucosaminyl transferase in Trypanosoma brucei. *Mol. Microbiol.* **71**, 478–491
8. Izquierdo, L., Acosta-Serrano, A., Mehlert, A., and Ferguson, M. A. J. (2015) Identification of a glycosylphosphatidylinositol anchor-modifying β1-3 galactosyltransferase in Trypanosoma brucei. *Glycobiology* **25**, 438–447
9. Kinoshita, T. (2020) Biosynthesis and biology of mammalian GPI-anchored proteins. *Open Biol.* **10**, 190290
10. Mayor, S., Menon, A. K., and Cross, G. A. M. (1992) Galactose-containing glycosylphosphatidylinositols in Trypanosoma brucei. *J. Biol. Chem.* **267**, 754–761
11. Leidich, S. D., Kostova, Z., Latek, R. R., Costello, L. C., Drapp, D. A., Gray, W., Fassler, J. S., and Orlean, P. (1995) Temperature-sensitive yeast GPI anchoring mutants gpi2 and gpi3 are defective in the synthesis of N -acetylglucosaminyl phosphatidylinositol. *J. Biol. Chem.* **270**, 13029–13035
12. Leidich, S. D., and Orlean, P. (1996) Gpi1, a Saccharomyces cerevisiae protein that participates in the first step in glycosylphosphatidylinositol anchor synthesis. *J. Biol. Chem.* **271**, 27829–27837
13. Yan, B. C., Westfall, B. A., and Orlean, P. (2001) Ynl038wp (Gpi15p) is the Saccharomyces cerevisiae homologue of human Pig-Hp and participates in the first step in glycosylphosphatidylinositol assembly. *Yeast* **18**, 1383–1389

14. Newman, H. A., Romeo, M. J., Lewis, S. E., Yan, B. C., Orlean, P., and Levin, D. E. (2005) Gpi19, the Saccharomyces cerevisiae homologue of mammalian PIG-P, is a subunit of the initial enzyme for glycosylphosphatidylinositol anchor biosynthesis. *Eukaryot. Cell.* **4**, 1801–1807
15. Murakami, Y., Siripanyaphinyo, U., Hong, Y., Tashima, Y., Maeda, Y., and Kinoshita, T. (2005) The initial enzyme for glycosylphosphatidylinositol biosynthesis requires PIG-Y, a seventh component. *Mol. Biol. Cell* **16**, 5236–5246
16. Watanabe, R., Inoue, N., Westfall, B. A., Taron, C. H., Orlean, P., Takeda, J., and Kinoshita, T. (1998) The first step of glycosylphosphatidylinositol biosynthesis is mediated by a complex of PIG-A, PIG-H, PIG-C and GPI1. *EMBO J.* **17**, 877–885
17. Inoue, N., Watanabe, R., Takeda, J., and Kinoshita, T. (1996) PIG-C, one of the three human genes involved in the first step of glycosylphosphatidylinositol biosynthesis is a homologue of Saccharomyces cerevisiae GPI2. *Biochem. Biophys. Res. Commun.* **226**, 193–199
18. Miyata, T., Takeda, J., Iida, Y., Yamada, N., Inoue, N., Takahashi, M., Maeda, K., Kitani, T., and Kinoshita, T. (1993) The cloning of PIG-A, a component in the early step of GPI-anchor biosynthesis. *Science* **259**, 1318–1320
19. Kamitani, T., Chang, H. M., Rollins, C., Waneck, G. L., and Yeh, E. T. H. (1993) Correction of the class H defect in glycosylphosphatidylinositol anchor biosynthesis in Ltk- cells by a human cDNA clone. *J. Biol. Chem.* **268**, 20733–20736
20. Watanabe, R., Murakami, Y., Marmor, M. D., Inoue, N., Maeda, Y., Hino, J., Kangawa, K., Julius, M., and Kinoshita, T. (2000) Initial enzyme for glycosylphosphatidylinositol biosynthesis requires PIG-P and is regulated by DPM2. *EMBO J.* **19**, 4402–4411
21. Kostova, Z., Rancour, D. M., Menon, A. K., and Orlean, P. (2000) Photoaffinity labelling with P3-(4-azidoanilido)uridine 5′-triphosphate identifies Gpi3p as the UDP-GlcNAc-binding subunit of the enzyme that catalyses formation of GlcNAc-phosphatidylinositol, the first glycolipid intermediate in glycosylphosphatidylinos. *Biochem. J.* **350**, 815–822
22. Kostova, Z., Yan, B. C., Vainauskas, S., Schwartz, R., Menon, A. K., and Orlean, P. (2003) Comparative importance *in vivo* of conserved glutamate residues in the EX7E motif retaining glycosyltransferase Gpi3p, the UDP-GlcNAc-binding subunit of the first enzyme in glycosylphosphatidylinositol assembly. *Eur. J. Biochem.* **270**, 4507–4514
23. Yadav, B., Bhatnagar, S., Ahmad, M. F., Jain, P., Pratyusha, V. A., Kumar, P., and Komath, S. S. (2014) First step of glycosylphosphatidylinositol (GPI) biosynthesis cross-talks with ergosterol biosynthesis and Ras signaling in Candida albicans. *J. Biol. Chem.* **289**, 3365–3382
24. Nagamune, K., Nozaki, T., Maeda, Y., Ohishi, K., Fukuma, T., Hara, T., Schwarz, R. T., Sutterlin, C., Brun, R., Riezman, H., and Kinoshita, T. (2000) Critical roles of glycosylphosphatidylinositol for Trypanosoma brucei. *Proc. Natl. Acad. Sci. U. S. A.* **97**, 10336–10341
25. Güther, M. L. S., Lee, S., Tetley, L., Acosta-Serrano, A., and Ferguson, M. A. J. (2006) GPI-anchored proteins and free GPI glycolipids of procyclic form Trypanosoma brucei are nonessential for growth, are required for colonization of the tsetse fly, and are not the only components of the surface coat. *Mol. Biol. Cell.* **17**, 5265–5274
26. Ferguson, M. A. J., Homans, S. W., Dwek, R. A., and Rademacher, T. W. (1988) Glycosyl-phosphatidylinositol moiety that anchors Trypanosoma brucei variant surface glycoprotein to the membrane. *Science* **239**, 753–759
27. Ferguson, M. A. J., Murray, P., Rutherford, H., and McConville, M. J. (1993) A simple purification of procyclic acidic repetitive protein and demonstration of a sialylated glycosyl-phosphatidylinositol membrane anchor. *Biochem. J.* **291**, 51–55
28. Treumann, A., Zitzmann, N., Hülsmeier, A., Prescott, A. R., Almond, A., Sheehan, J., and Ferguson, M. A. J. (1997) Structural characterisation of two forms of procyclic acidic repetitive protein expressed by procyclic forms of Trypanosoma brucei. *J. Mol. Biol.* **269**, 529–547
29. Field, M. C., Menon, A. K., and Cross, G. A. M. (1991) A glycosylphosphatidylinositol protein anchor from procyclic stage Trypanosoma brucei: Lipid structure and biosynthesis. *EMBO J.* **10**, 2731–2739
30. Masterson, W. J., Doering, T. L., Hart, G. W., and Englund, P. T. (1989) A novel pathway for glycan assembly: Biosynthesis of the glycosylphosphatidylinositol anchor of the trypanosome variant surface glycoprotein. *Cell* **56**, 793–800
31. Menon, A. K., Schwarz, R. T., Mayor, S., and Cross, G. A. M. (1990) Cell-free synthesis of glycosyl-phosphatidylinositol precursors for the glycolipid membrane anchor of Trypanosoma brucei variant surface glycoproteins. Structural characterization of putative biosynthetic intermediates. *J. Biol. Chem.* **265**, 9033–9042
32. Menon, A. K., Mayor, S., and Schwarz, R. T. (1990) Biosynthesis of glycosyl-phosphatidylinositol lipids in Trypanosoma brucei: Involvement of mannosyl-phosphoryldolichol as the mannose donor. *EMBO J.* **9**, 4249–4258
33. Field, M. C., Menon, A. K., and Cross, G. A. M. (1992) Developmental variation of glycosylphosphatidylinositol membrane anchors in Trypanosoma brucei. *In vitro* biosynthesis of intermediates in the construction of the GPI anchor of the major procyclic surface glycoprotein. *J. Biol. Chem.* **267**, 5324–5329
34. Field, M. C., Menon, A. K., and Cross, G. A. M. (1991) Developmental variation of glycosylphosphatidylinositol membrane anchors in Trypanosoma brucei: Identification of a candidate biosynthetic precursor of the glycosylphosphatidylinositol anchor of the major procyclic stage surface glycoprotein. *J. Biol. Chem.* **266**, 8392–8400
35. Nakanishi, M., Karasudani, M., Shiraishi, T., Hashida, K., Hino, M., Ferguson, M. A. J., and Nomoto, H. (2014) TbGT8 is a bifunctional glycosyltransferase that elaborates N-linked glycans on a protein phosphatase AcP115 and a GPI-anchor modifying glycan in Trypanosoma brucei. *Parasitol. Int.* **63**, 513–518
36. Montagna, G. N., Cremona, M. L., Paris, G., Amaya, M. F., Buschiazzo, A., Alzari, P. M., and Frasch, A. C. C. (2002) The trans-sialidase from the African trypanosome Trypanosoma brucei. *Eur. J. Biochem.* **269**, 2941–2950
37. Montagna, G. N., Donelson, J. E., and Frasch, A. C. C. (2006) Procyclic Trypanosoma brucei expresses separate sialidase and trans -sialidase enzymes on its surface membrane. *J. Biol. Chem.* **281**, 33949–33958
38. Smith, T. K., and Bütikofer, P. (2010) Lipid metabolism in Trypanosoma brucei. *Mol. Biochem. Parasitol.* **172**, 66–79
39. [preprint] Ji, Z., Tinti, M., and Ferguson, M. A. J. (2020) Proteomic identification of the UDP-GlcNAc : PI α1-6 GlcNAc-transferase subunits of the glycosylphosphatidylinositol biosynthetic pathway of Trypanosoma brucei. *bioRxiv*. https://doi.org/10.1101/2020.12.16.423025
40. Mazhari-Tabrizi, R., Eckert, V., Blank, M., Müller, R., Mumberg, D., Funk, M., and Schwarz, R. T. (1996) Cloning and functional expression of glycosyltransferases from parasitic protozoans by heterologous complementation in yeast: The dolichol phosphate mannose synthase from Trypanosoma brucei brucei. *Biochem. J.* **316**, 853–858
41. Verchère, A., Cowton, A., Jenni, A., Rauch, M., Häner, R., Graumann, J., Bütikofer, P., and Menon, A. K. (2021) Complexity of the eukaryotic dolichol-linked oligosaccharide scramblase suggested by activity correlation profiling mass spectrometry. *Sci. Rep.* **11**, 1411
42. Stevens, V. L., and Raetz, C. R. H. (1991) Defective glycosyl phosphatidylinositol biosynthesis in extracts of three Thy-1 negative lymphoma cell mutants. *J. Biol. Chem.* **266**, 10039–10042
43. Vassella, E., Bütikofer, P., Engstler, M., Jelk, J., and Roditi, I. (2003) Procyclin null mutants of Trypanosoma brucei express free glycosylphosphatidylinositols on their surface. *Mol. Biol. Cell.* **14**, 1308–1318
44. Roditi, I., Carrington, M., and Turner, M. (1987) Expression of a polypeptide containing a dipeptide repeat is confined to the insect stage of Trypanosoma brucei. *Nature* **325**, 272–274
45. Bütikofer, P., Ruepp, S., Boschung, M., and Roditi, I. (1997) "GPEET" procyclin is the major surface protein of procyclic culture forms of Trypanosoma brucei brucei strain 427. *Biochem. J.* **326**(Pt 2), 415–423
46. Roditi, I., Furger, A., Ruepp, S., Schürch, N., and Bütikofer, P. (1998) Unravelling the procyclin coat of Trypanosoma brucei. *Mol. Biochem. Parasitol.* **91**, 117–130
47. Vassella, E., Van Den Abbeele, J., Bütikofer, P., Renggli, C. K., Furger, A., Brun, R., and Roditi, I. (2000) A major surface glycoprotein of Trypanosoma brucei is expressed transiently during development and can be regulated post-transcriptionally by glycerol or hypoxia. *Genes Dev.* **14**, 615–626

48. Signorell, A., Jelk, J., Rauch, M., and Bütikofer, P. (2008) Phosphatidylethanolamine is the precursor of the ethanolamine phosphoglycerol moiety bound to eukaryotic elongation factor 1A. *J. Biol. Chem.* **283**, 20320–20329
49. Güther, M. L. S., Beattie, K., Lamont, D. J., James, J., Prescott, A. R., and Ferguson, M. A. J. (2009) Fate of glycosylphosphatidylinositol (GPI)-less procyclin and characterization of sialylated non-GPI-anchored surface coat molecules of procyclic-form Trypanosoma brucei. *Eukaryot. Cell* **8**, 1407–1417
50. Gottier, P., González-Salgado, A., Menon, A. K., Liu, Y. C., Acosta-Serrano, A., and Bütikofer, P. (2017) RFT1 protein affects glycosylphosphatidylinositol (GPI) anchor glycosylation. *J. Biol. Chem.* **292**, 1103–1111
51. Imhof, S., Vu, X. L., Bütikofer, P., and Roditi, I. (2015) A glycosylation mutant of Trypanosoma brucei links social motility defects *in vitro* to impaired colonization of tsetse flies *in vivo*. *Eukaryot. Cell* **14**, 588–592
52. Imhof, S., Knüsel, S., Gunasekera, K., Vu, X. L., and Roditi, I. (2014) Social motility of African trypanosomes is a property of a distinct life-cycle stage that occurs early in tsetse fly transmission. *PLoS Pathog.* **10**, e1004493
53. Vassella, E., Oberle, M., Urwyler, S., Renggli, C. K., Studer, E., Hemphill, A., Fragoso, C., Bütikofer, P., Brun, R., and Roditi, I. (2009) Major surface glycoproteins of insect forms of Trypanosoma brucei are not essential for cyclical transmission by tsetse. *PLoS One* **4**, e4493
54. Partridge, J. D., and Harshey, R. M. (2013) Swarming: Flexible roaming plans. *J. Bacteriol.* **195**, 909–918
55. Madukoma, C. S., Liang, P., Dimkovikj, A., Chen, J., Lee, S. W., Chen, D. Z., and Shrout, J. D. (2019) Single cells exhibit differing behavioral phases during early stages of pseudomonas aeruginosa swarming. *J. Bacteriol.* **201**, e00184-19
56. Islam, S. T., Alvarez, I. V., Saïdi, F., Guiseppi, A., Vinogradov, E., Sharma, G., Espinosa, L., Morrone, C., Brasseur, G., Guillemot, J. F., Benarouche, A., Bridot, J. L., Ravicoularamin, G., Cagna, A., Gauthier, C., *et al.* (2020) Modulation of bacterial multicellularity via spatio-specific polysaccharide secretion. *PLoS Biol.* **18**, e3000728
57. Kirchner, N., Cano-Prieto, C., Schulz-Fincke, A.-C., Gütschow, M., Ortlieb, N., Moschny, J., Niedermeyer, T. H. J., Horak, J., Lämmerhofer, M., van der Voort, M., Raaijmakers, J. M., and Gross, H. (2021) Discovery of thanafactin A, a linear, proline-containing octalipopeptide from Pseudomonas sp. SH-C52, motivated by genome mining. *J. Nat. Prod.* **84**, 101–109
58. He, C. Y., Ho, H. H., Malsam, J., Chalouni, C., West, C. M., Ullu, E., Toomre, D., and Warren, G. (2004) Golgi duplication in Trypanosoma brucei. *J. Cell Biol.* **165**, 313–321
59. Farine, L., Niemann, M., Schneider, A., and Bütikofer, P. (2015) Phosphatidylethanolamine and phosphatidylcholine biosynthesis by the Kennedy pathway occurs at different sites in Trypanosoma brucei. *Sci. Rep.* **5**, 16787
60. Hong, Y., Ohishi, K., Watanabe, R., Endo, Y., Maeda, Y., and Kinoshita, T. (1999) GPI1 stabilizes an enzyme essential in the first step of glycosylphosphatidylinositol biosynthesis. *J. Biol. Chem.* **274**, 18582–18588
61. Levin, D. E., and Stamper, R. J. (2009) Chapter 2 the N-acetylglucosamine-PI transfer reaction, the GlcNAc-PI transferase complex, and its regulation. In *Enzymes* (Vol 26,. Cold Spring Harbor Press, New York, NY: 31–47
62. Engstler, M., Reuter, G., and Schauer, R. (1992) Purification and characterization of a novel sialidase found in procyclic culture forms of Trypanosoma brucei. *Mol. Biochem. Parasitol.* **54**, 21–30
63. Yadav, A., Singh, S. L., Yadav, B., and Komath, S. S. (2014) Saccharomyces cerevisiae Gpi2, an accessory subunit of the enzyme catalyzing the first step of glycosylphosphatidylinositol (GPI) anchor biosynthesis, selectively complements some of the functions of its homolog in Candida albicans. *Glycoconj. J.* **31**, 497–507
64. Beneke, T., Madden, R., Makin, L., Valli, J., Sunter, J. D., and Gluenz, E. (2017) A CRISPR Cas9 high-throughput genome editing toolkit for kinetoplastids. *R. Soc. Open Sci.* **4**, 170095
65. Shaw, S., Knüsel, S., Hoenner, S., and Roditi, I. (2020) A transient CRISPR/Cas9 expression system for genome editing in Trypanosoma brucei. *BMC Res. Notes* **13**, 268
66. Dean, S., Sunter, J. D., Wheeler, R. J., Hodkinson, I., Gluenz, E., and Gull, K. (2015) A toolkit enabling efficient, scalable and reproducible gene tagging in trypanosomatids. *Open Biol.* **5**, 140197
67. Serricchio, M., and Bütikofer, P. (2013) Phosphatidylglycerophosphate synthase associates with a mitochondrial inner membrane complex and is essential for growth of Trypanosoma brucei. *Mol. Microbiol.* **87**, 569–579
68. Field, M. C., and Menon, A. K. (1992) Biosynthesis of glycosylphospahtidylinositol membrane protein anchors. In: Hooper, N. M., Turner, A. J., eds. *Lipid Modification of Proteins: A Practical Approach*, Oxford University Press, Oxford: 155–190
69. Laemmli, U. K. (1970) Cleavage of structural proteins during the assembly of the head of bacteriophage T4. *Nature* **227**, 680–685
70. Bütikofer, P., Vassella, E., Ruepp, S., Boschung, M., Civenni, G., Seebeck, T., Hemphill, A., Mookherjee, N., Pearson, T. W., and Roditi, I. (1999) Phosphorylation of a major GPI-anchored surface protein of Trypanosoma brucei during transport to the plasma membrane. *J. Cell Sci.* **112**(Pt 1), 1785–1795
71. Florini, F., Naguleswaran, A., Gharib, W. H., Bringaud, F., and Roditi, I. (2019) Unexpected diversity in eukaryotic transcription revealed by the retrotransposon hotspot family of Trypanosoma brucei. *Nucleic Acids Res.* **47**, 1725–1739
72. Serricchio, M., and Bütikofer, P. (2012) An essential bacterial-type cardiolipin synthase mediates cardiolipin formation in a eukaryote. *Proc. Natl. Acad. Sci. U. S. A.* **109**, E954–E961